QUANTIFYING THE BATHYMETRY OF THE LOWER COLORADO RIVER BASIN, ARIZONA, WITH AIRBORNE LIDAR

Kutalmis Saylam*, John R. Hupp, and Aaron R. Averett

Near Surface Observatory
Bureau of Economic Geology
John A. and Katherine G. Jackson School of Geosciences
The University of Texas at Austin
Austin, Texas 78758
USA

* Corresponding author:

Kutalmis Saylam

Kutalmis.Saylam@beg.utexas.edu

PURPOSE

Airborne Lidar bathymetry (ALB) is an effective and advanced technology for mapping and characterizing shallow coastal water zones as well as inland freshwater basins such as rivers and lakes. The ability of light beams to detect and traverse shallow water-columns has provided valuable information about unmapped and often poorly understood coastal and inland water bodies of the world. In January 2016, we conducted airborne Lidar surveys in the lower Colorado River, near Parker, Arizona. The purpose of the project was to determine and map the geomorphology of the river basin, including the water-bottom surface. The project covered an area of approximately 260 km^2 of the river, with varying terrain altitude, water clarity, depth, and flow conditions. The survey was conducted using two separate airborne Lidar systems: AHAB Chiroptera and Trimble Harrier 68i. Chiroptera was used to survey the river and immediate shoreline, and Harrier acquired data to map overall river topography. Real-time in situ measurements to understand water clarity (turbidity) were completed onsite, and dual-beam sonar data were captured to complement and verify Lidar bathymetry in the deeper parts of the riverbed. This paper discusses the bathymetric findings.

KEYWORDS: Lidar, river bathymetry, water clarity, remote sensing, sonar

INTRODUCTION

In January 2016, researchers from the Bureau of Economic Geology (Bureau) and staff from Surveying and Mapping, LLC (SAM) mobilized to conduct airborne Lidar surveys in the lower Colorado River basin, in the states of Arizona and California. Because of contractual obligations, two separate airborne Lidar systems were used concurrently: the Bureau used the Airborne Hydrography AB (AHAB) Chiroptera for bathymetry, and SAM used the Trimble Harrier 68i for topography.

The Bureau owns and operates the Chiroptera, which was built for the Bureau in 2012. This first-of-its-kind system has two scanners (red and green wavelength) and uses a green wavelength of 0.5 µm for bathymetric data collection, from an effective range of 400 m altitude. The system acquires data by continous waveform signals and interpolates individual returns. Chiroptera directs the light beam with a constant (non-user-configurable) incident angle (from vertical) of 28° in a forward/backward direction to 40° sideways with an elliptical pattern (Palmer scanner). SAM maintains and operates a Trimble Harrier 68i system with a 1 µm (near-infrared) wavelength for topographical data collection. The system acquires data with a maximum repetition rate of 400 kHz and has an adjustable scanning pattern that operates with a rotating polygon motion.

The final products, a merged digital elevation model (DEM) and orthophotography, were intended to facilitate understanding of Colorado River basin geomorphology. In 2015, the river was classified as the most endangered in the United States. The river runs through seven states and Mexico (**Figure 1**), providing water for nearly 40 million people and irrigating close to 2 million hectares of land before it drains into the Sea of Cortez. Warmer weather, less snowfall, and more than one hundred dams built into the river's path have reduced its water volume considerably, placing significant stress on its ecosystem and impacting fish and wildlife habitat as well as the river's $26 billion recreational economy. Water flow is expected to decrease by 10 to 30 percent by 2050 (Sinjin and Roger, 2015).

A recent article (Saylam, 2016) provides an overall look at the project; this paper concentrates on bathymetric findings on the river as quantified by different classes of Lidar returns and sonar measurements.

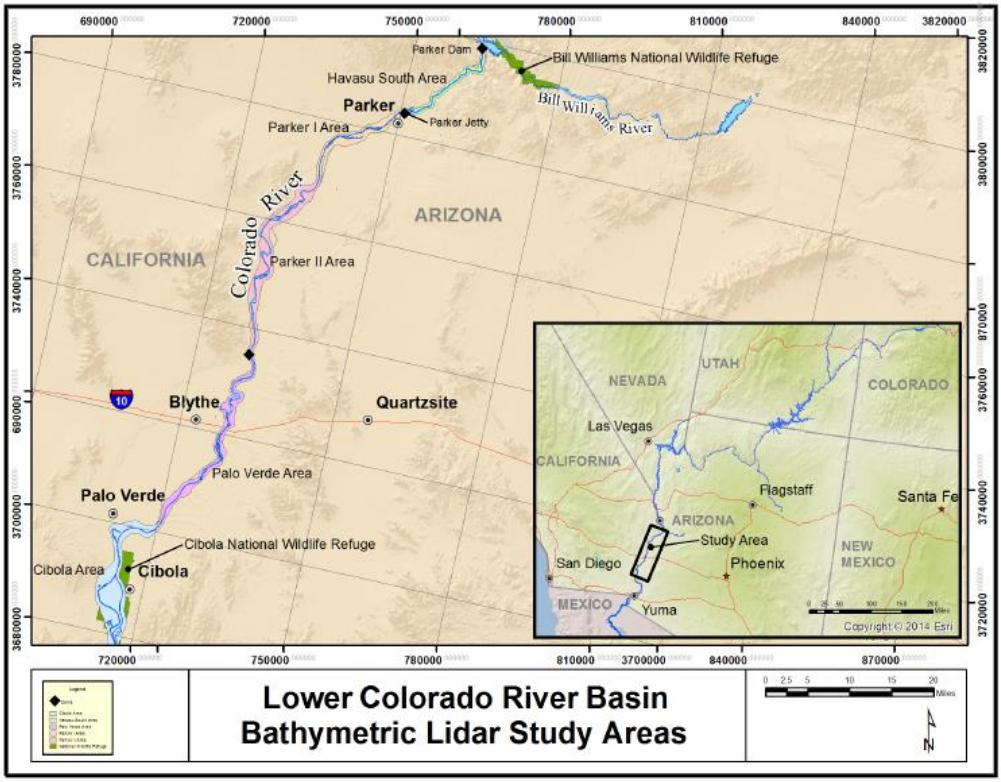

Figure 1: Airborne survey location; upper river near Parker Dam, Arizona, to lower river near Cibola, California.

MATERIALS AND METHODS

Essential qualities for airborne Lidar surveys are precision, detail, and cost effectiveness. Because of the complex nature of such surveys, successful project completion requires understanding and careful implementation of quality assurance (QA) procedures (Saylam, 2009**)**. This is especially true of airborne Lidar bathymetry (ALB) surveys, for which there are highly variable environmental and logistical considerations. In situ measurements may provide good understanding of conditions and expectations; however, in remote locations of the world, such practices may not be feasible or even possible because of environmental restrictions. In general, the following should be taken into account for a successful ALB survey:

- **Depth of water-column**: Capabilities of ALB systems vary from model to model. They have different depth-penetrating capabilities limited by their hardware, and rely on laser-power energy, aperture size, optical bandwidth, time and travel measurement efficiency, among other considerations (Guenther et al., 2000**)**. ALB surveys should be planned with respect to system capabilities.

- **Water clarity**: The green wavelength is easily attenuated by adverse water-body health. Sediments, dissolved organic and inorganic materials, algae, environmental pollution, and all other contaminants influence overall water quality **(**Saylam et al., 2017**)**. As a rule of thumb, we expect 1–3 times the Secchi disk depth *(SD)* of Lidar penetration into the water-column. Chiroptera is rated for 1.5 x *SD*.

- **Terrain and environmental conditions**: These conditions are often overlooked but possibly essential for a successful ALB survey. The flat and calm waters of inland regions may require fewer QA considerations compared to surveys in coastal or mountainous regions.

- **Expertise with bathymetric Lidar processing**: Bathymetric Lidar data proceesing is significantly different and more demanding compared to topographical Lidar data proceesing. The former requires additional tools and applications, knowledge base and additional efforts for creating accurate final products. Analysts need to understand and study the formation of waveform signals and their direct impact on final deliverables.

In this study, we completed measurements to understand water-clarity conditions of the river simultaneously with ALB data acquisition. Additionally, in the deeper parts of the river, where we expected the Lidar signal to become exhausted at certain depths, we acquired river-based measurements to correlate with Lidar returns.

Airborne survey preparation

ALB missions were planned to cover approximately 260 km^2 of the river area, with varying terrain altitude, water clarity, depth, and flow conditions. Because of the highly varying ground altitude at the northern end of the survey area, with mountain peaks higher than 500 m, critical attention was given to flight planning for safe aircraft maneuvering and maintaining a steady swath on the ground. Discussions were also held with Parker Dam authorities to ensure that airborne missions were conducted during periods of low discharge.

Parker Dam, located at the northern end of the survey area, adjusts the water level and flow of the river in the lower basin, causing the water level to fluctuate daily and annually. According to (USGS, 2016), the mean monthly discharge rate is 146 m^3/sec for the month of January, which is significantly lower compared to the mean yearly flow rate of 252 m^3/sec. During the airborne missions, the discharge rates varied, from 65 m^3/sec in the morning to 230 m^3/sec in late afternoon (**Figure 2**), causing the Parker Dam gauge height to change by 1.1 m (USGS, 2016). We confirmed this variation with Lidar, measuring up to 1.15 m difference in the water-surface elevation between two survey dates and times (morning and afternoon). Low discharge rates reduce the water level and flow of the river, and contribute to lower turbidity levels.

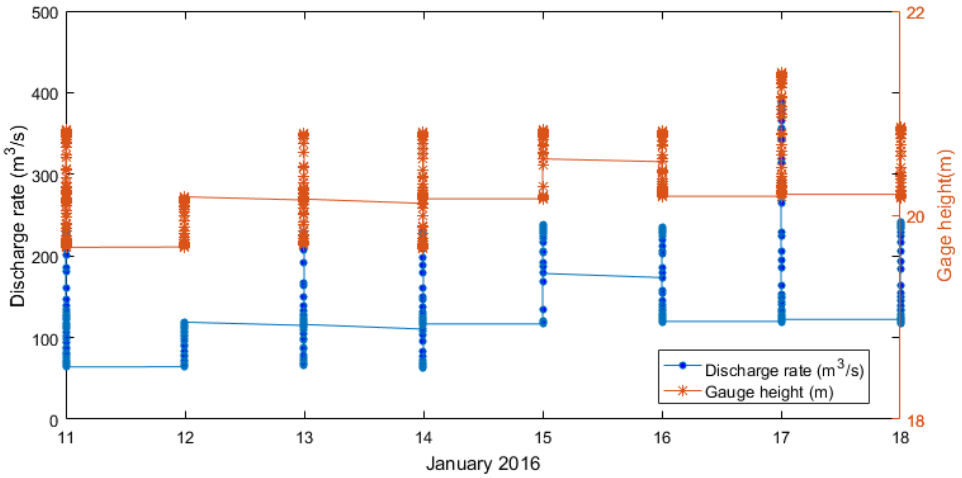

Figure 2: Water discharge rate (m^3/s) and gauge height (m) at Parker Dam during week of airborne survey.

Survey calibration

For ground-truthing purposes, a number of GNSS receivers overlapping each other were set up by SAM staff. Online positioning user services (OPUS and CSRS-PPP) were used to correct the static GPS data collected for each day. Continuously operating reference station (CORS) data from local areas (AZLH, GMPK) were also downloaded for backup purposes.

A total of 46 ground control points (GCPs) were acquired over the airport runway surface at the Avi Suquilla airport (P-20) using a real-time kinematic GPS system. Both Lidar systems were flown over the airport multiple times and in opposing directions to estimate boresight-calibration values and slant-range (vertical elevation) bias. For slant-range measurement, every Lidar return registered in a 1-m radius of a GCP was extracted to build a localized triangulated irregular network (TIN) patch. The elevation of the TIN was compared against a selected GCP to determine vertical bias. This process was applied to all three scanners for a seamless integration of data sets. We calculated the R-squared value at 0.9993 and the root-mean-square error (RMSE) at between 1 to 2 cm. **Figure 3** displays the goodness of fit between the Trimble scanner and both Chiroptera scanners, and between the scanners and the GCPs.

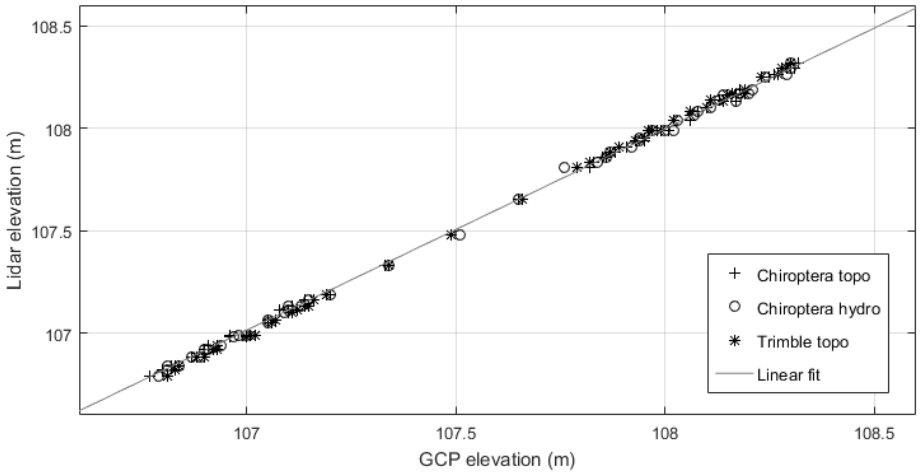

Figure 3: Goodness of fit among Lidar scanners to ground control points and to each other.

Bathymetric Lidar and waveform analysis

ALB and waveform analysis in shallow and inland waters (e.g., lakes and rivers) is an area of active research **(**Kinzel et al., 2013; Bouhdaoui et al., 2014; Pan et al., 2015; Wang et al., 2015**)**. Waveforms, with their potential to provide information about water-column and bottom characteristics of a water body, are a valuable source of data. In the bathymetric framework, the visible (green wavelength) light beam traverses the air–water interface and propagates in the water-column until the bottom is reached. If the beam is not attenuated in the water-column, backscatter reaches back to the receiver, indicating the surface and bottom locations with distinctive peaks in the waveform (**Figure 4**). Water-column depth is calculated based on the number of samples between peaks, where *d_m* = distance in meters, *d_s* = distance in number of samples, *f_s* = sample frequency (1.8 GHz), *c* = speed of light, and *n* = refractive index of water ($d\_m = (c\ d\_s)/(2nf\_s)$). The refraction value varies with water temperature, salinity, and wavelength. In this study, the average water temperature was measured at 10°C, which corresponds to 1.3376 with no salinity for 0.5 µm of wavelength (Quan and Fry, 1995).

In shallow and calm waters, surface and bottom detection within the backscatter may be challenging. The surface peak may disappear altogether, resulting in a broader and weaker single peak (Allouis et al., 2010**)**. In such cases, a simulated water-surface is composed by using NIR beams from the topographical scanner, which are reflected off the water-surface, generally with more amplitude. Because linear simulation created by NIR beams may not represent the surface correctly, we analysed both return types. Class 0 represents the simulated surface, Class 5 are regular returns as registered by the bathymetric scanner. For water-bottom detection analysis, we studied Classes 7 and 10 (regular and enhanced algorithm products) and compared the findings with sonar readings. Class 10 returns are expected to register deeper returns because of an enhanced algorithm that picks up weaker returns in the waveform (**Figure 5**). Returns were output and classified by the Lidar Survey Suite (LSS v2.3) application with user-set thresholds; classes are proprietary for LAS 1.2.

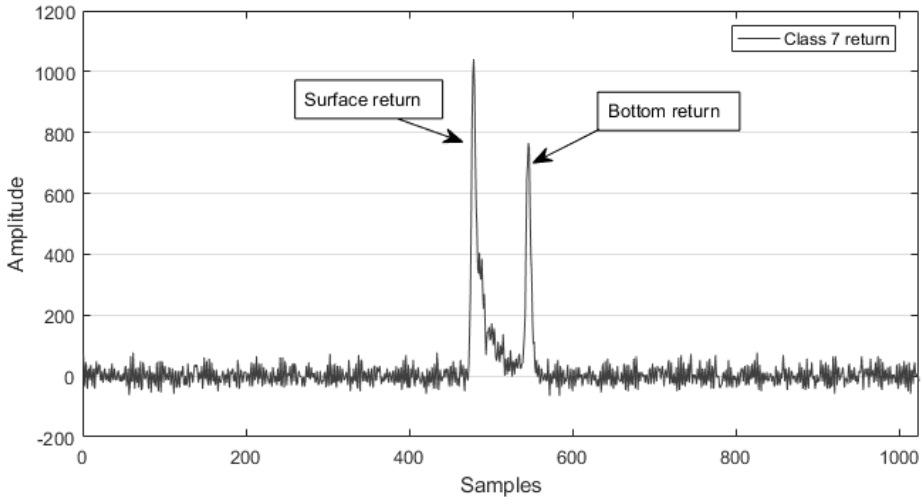

Figure 4: Waveform example with distinctive water-surface and bottom returns (Class 7).

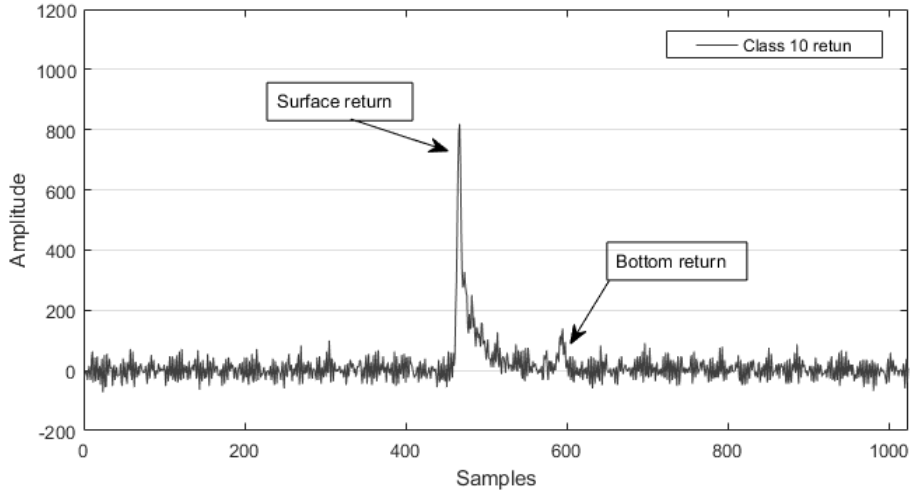

Figure 5: Waveform example with strong water-surface and weak bottom returns (Class 10).

Sonar-data acquisition

Sonar data provide invaluable information for understanding the depth of the water-column, where physical measurements with traditional methods are not practical. We collected 4,200 individual sonar waypoints in conjunction with an ALB survey in the deeper areas of the river. Garmin 74dv collects data up to 200 kHz with dual-beam technology and in freshwater bodies; effective depth range is rated at 700 m. We compared sonar readings with available Lidar returns, although a slight divergence was expected in the deeper parts of the river due to the lack of an inertial navigation system (INS). Our testing to understand the accuracy of the sonar unit in a lab environment produced close-fitting results, where standard deviation measured was 2.7 cm at a depth of 11.8 m, which is very comparable to deeper sections of the river. However, there are conditions that will effect the accuracy of sonar measurement in the river bed, movement and surface choppiness as the major variables.

Data were acquired across 13 transects along the deeper pockets of the river within the same time frame that airborne missions were completed. Sonar readings included time, location, depth, and water temperature. The shallowest point was 38 cm; 17.01 m was the deepest of all readings. Mean water temperature was recorded at 10°C. For quantification purposes, we examined the accuracy of sonar data versus water-bottom LSS-derived Lidar returns (Classes 7 and 10). Using the Delauney triangulation algorithm, we built a TIN patch of Lidar returns that are within 1 m of a sonar reading, excluding returns farther away than 1 m in vertical height and those exceeding 30° on a slope. **Figure 6** illustrates a sample transect where Lidar returns were extinct at an approximate depth of 9 m, and sonar readings reached the bottom of the river at approximately 13 m depth.

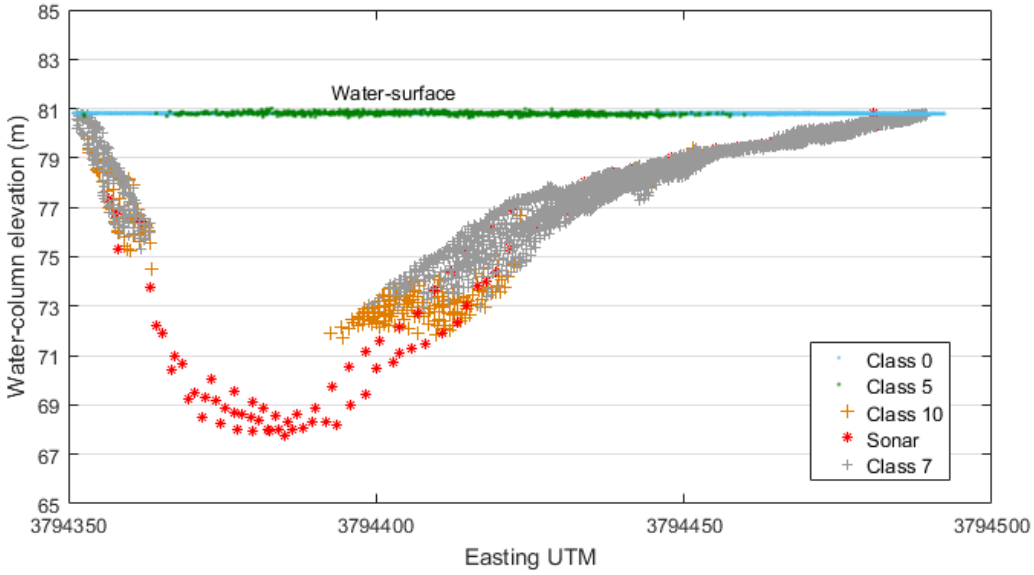

Figure 6: Transect cross-section sample with Lidar and sonar returns.

Water-clarity measurements

Turbidity is an expression of the optical property that causes light to be scattered and absorbed rather than transmitted in straight lines through the sample (Jethra, 1993). In this study, we measured turbidity with a portable field turbidimeter that complied with Environmental Protection Agency (EPA) method 180.11 **(**O'Dell, 1993**)**. The Hach 2100Q measures turbidity between 0 and 1,000 nephelometric turbidity units (NTU), with a resolution of 0.01 NTU. Measurements were completed throughout the river in conjunction with the airborne surveys to gain a direct understanding of ALB survey expectations. The average reading was 0.41 NTU in the northern sections of the river, which indicated overall low levels of turbidity in the water-column. In the south, the river is shallower, running through a desertlike environment and losing much of its water to irrigation. These conditions contributed to higher turbidity levels of up to 6.25 NTU and created difficulties for Lidar bathymetry. In this study, we focused on areas where we collected sonar measurements and excluded shallow river areas in the south with higher turbidity.

FINDINGS

We examined 16 transects and analyzed water-surface and water-bottom returns as they were output from LSS. For water-surface detection, Class 0 represents the simulated surface level, which is mostly linear, as detected by NIR wavelength. Class 5 returns, which follow natural water-surface patterns, are confirmed by the green-wavelength surface-detection algorithm. An average transect (150 m wide) registered 62,160 returns for Class 0, whereas only 985 returns output as Class 5. The discrepancy in the number of returns is the product of efficiency in red versus green wavelength-detection algorithms in clear and reflective waters, as well as the output thresholds set within LSS for peak and slope detection. It is possible to increase the number of Class 5 returns by adjusting backscatter and amplitude thresholds within the LSS application. However, this was not an essential exercise in our study because of the flat and calm water surface of the river.

Our findings indicated that LSS algorithms produced robust and very well fitting results between these two water-surface classes, especially in less-turbid and deeper-water conditions, where overall difference and standard deviation was only 3 cm. Shallower and more-turbid water conditions (transects 14 to 16) produced slightly higher

numbers, whereas Class 0 returns were 10 cm lower as an average compared to those of Class 5. Overall RMSE was 12 cm and R-squared value was calculated at 0.9989, which denotes a very predictable fit (**Figure 7).**

For water-bottom detection, we analyzed LSS-derived Classes 7 and 10. An average of 39,950 returns were registered as Class 7; Class 10 averaged 8,420 returns for each area of interest. The Class 10 algorithm, built to register less-distinctive return peaks in turbid water-columns, was effective in registering deeper water-columns. In deeper and less-turbid areas of the river (transects 1 to 13), Class 10 recorded an average improvement of 81 cm (7.99 m versus 8.80 m), which is a considerable achievement. **Figure 8** illustrates an empirical cumulative function graph (CDF) of the water-bottom classes where each class either registered the river bottom, or the water-column depth before they were attenuated. **Figure 9** shows the water-surface and water-bottom representation at each transect as they were output by LSS. It is evident that Class 10 registered deeper water depths at most locations. However, Class 7 and Class 10 returns may not represent the actual water-bottom, as the returns may have attenuated before the Lidar beams reached to the bottom. For example, we measured a discrepancy of 7.84 m at the third transect, between Class 10 and the sonar measurement, where Lidar returned a depth of 9.17 m and attenuated. The shallow and more-turbid parts of the river (transects 14 to 16) produced less-significant results between the water-bottom classes; improvement was only 13 cm.

A total of 1,343 point-to-point comparisons were calculated for sonar measurement findings. We also plotted our findings with a CDF graph (**Figure 10**). The graph reveals that sonar readings mostly matched Lidar returns from a water-surface to water-bottom depth of approximately 4.5 m (77.5 m water-column elevation). In deeper parts of the river, the majority of sonar readings registered slightly higher than Lidar returns, indicating deeper bottoms, whereas Lidar returns were attenuated. Overall, Class 7 returns had a better fit with sonar readings compared to Class 10 returns (**Table 1**).

Table 1: Sonar versus water-bottom LSS-derived returns

Sonar versus	# of samples	Mean difference (m)	Standard deviation (m)	R-squared	RMSE (m)
Class 7	843	0.14	0.37	0.9750	0.326
Class 10	500	0.19	0.39	0.9691	0.333

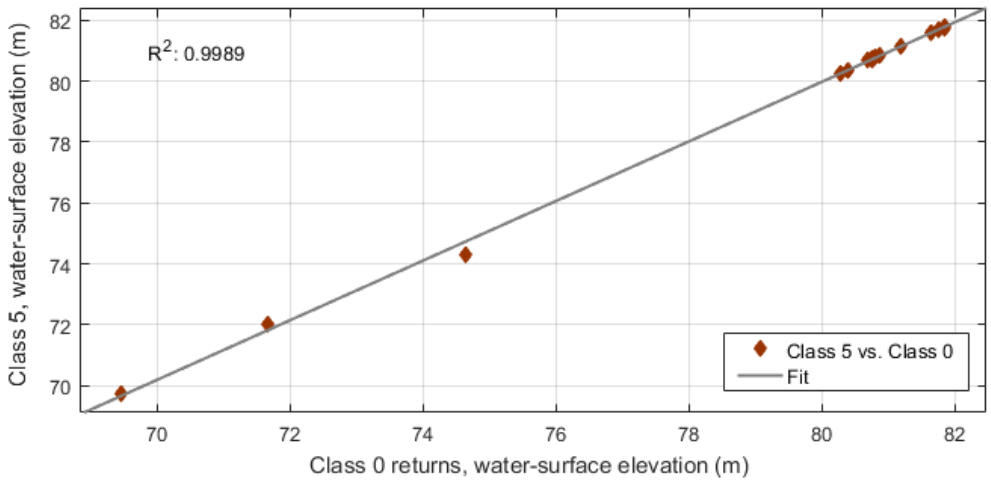

Figure 7: Water-surface representation, Class 0 versus Class 5.

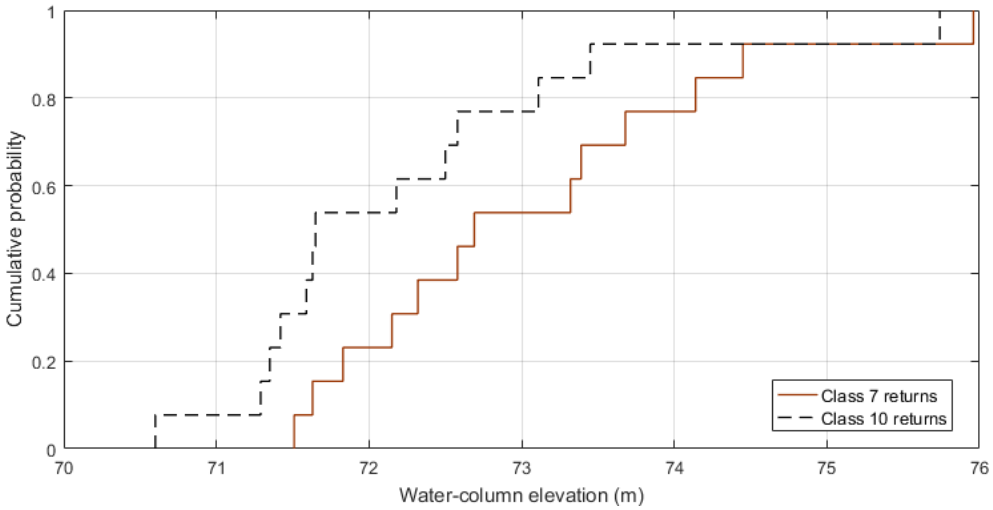

Figure 8: Emprical cumulative probability of water-bottom classes; Classes 7 and 10.

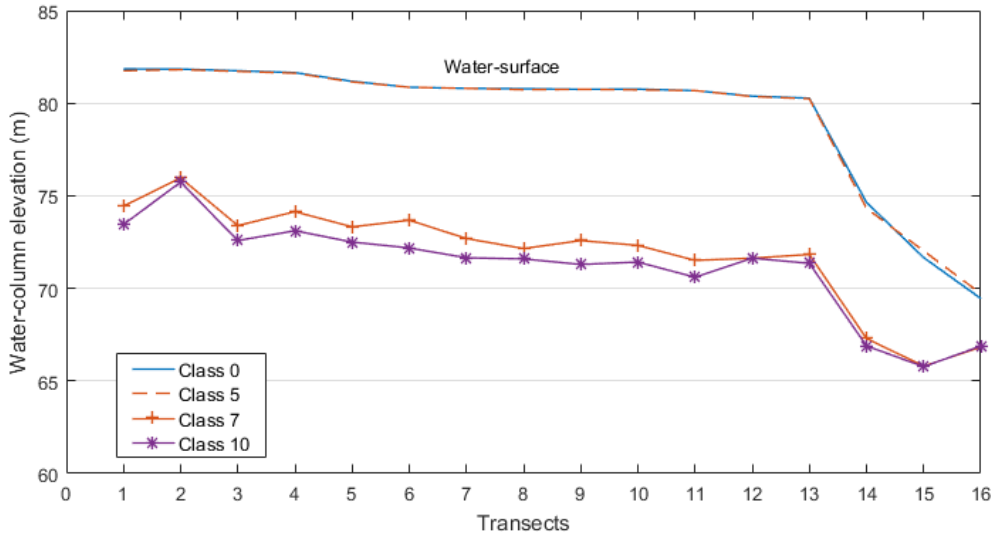

Figure 9: Comparison of LSS-derived water-surface and water-bottom classes.

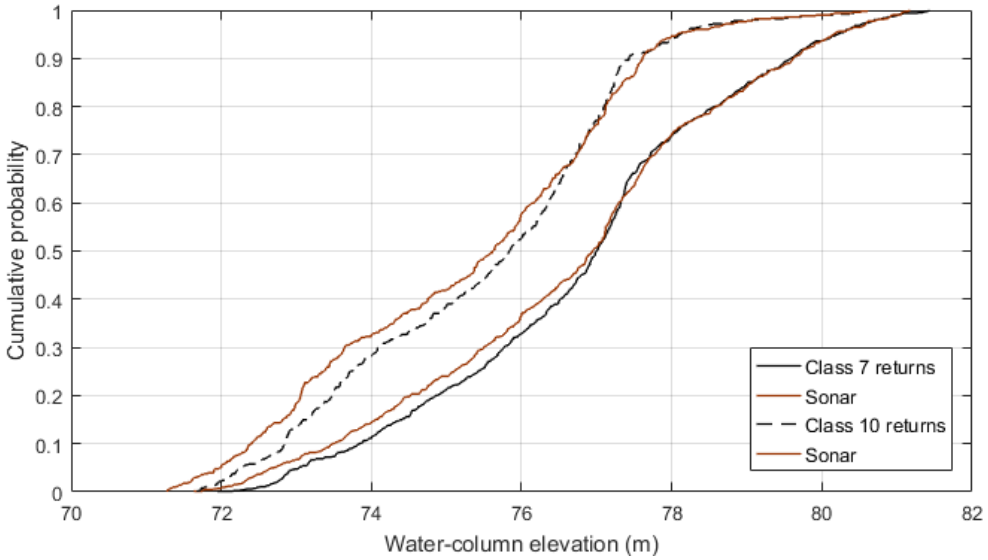

Figure 10: Empirical cumulative function of sonar versus water-bottom classes 7 and 10.

CONCLUSION AND DISCUSSION

The bathymetric findings of the lower Colorado River basin survey have proven again that Lidar can be an effective and extremely capable tool for revealing the complex geomorphology of a river. The technology behind emitting light beams that can penetrate as deep as 10 m into a water-column produce many opportunities for advancement in mapping, geology, hydrogeology, geomatics, and many other related science fields.

Turbidity in the water-column is the major challenge for ALB surveys, and advancing beyond this obstacle has been a slow process. As illustrated in this study, an overall improvement of 81 cm deeper penetration using a tighter threshold in return-extraction algorithms (Class 7 versus Class 10) should be considered an achievement, particularly in survey locations like the Colorado River, where water flows deeply and swiftly in a desertlike environment. However, Class 7 returns produced better fitting results to sonar measurements, indicating a more stable medium.

We expect to expand the findings of this project to other similar inland water bodies and coastal areas. Use of sonar proved to be a valuable resource, and its application is strongly recommended for similar ALB surveys. However, for choppy waters, an INS integration would be essential to produce more accurate results. It is also strongly recommended to conduct in situ water clarity measurements, preferably before and during the airborne data acquisition stages. Examining and planning around the variable environmental conditions (e.g., rain, wind, seasonal changes, etc.) at the survey location would increase the chances of completing ALB surveys successfully.

As a further continuation to this study, we will examine the Lidar returns and their robustness in deep water conditions where beams are attenuated before they reach the bottom. We expect to find varying results, depending on the environmental and various other conditions, and we will attempt to correlate our results with sonar for further understanding and quantifying the Lidar bathymetry.

ACKNOWLEDGEMENT

The project was administered by Allied GIS of Anchorage, Alaska. Surveying and Mapping LLC of Austin, Texas staff provided ground truthing along the survey area. Flight services were provided by Aspen Helicopters of Oxnard, California. BEG researcher Aaron Averett operated the Lidar sensor, and John Hupp supervised the field work and data processing. Dr. Jeffrey Paine, John Andrews and Tiffany Caudle provided valuable overall project assistance in Austin, Texas. Stephanie Jones revised and edited the paper to comply with conference proceedings language quality.

REFERENCES

Allouis, T., Bailly, J.-S., Pastol, Y., Le Roux, C., 2010. Comparison of Lidar waveform processing methods for very shallow water bathymetry using Raman, near-infrared and green signals. Earth Surf. Process. Landf. n/a-n/a. doi:10.1002/esp.1959

Bouhdaoui, A., Bailly, J.-S., Baghdadi, N., Abady, L., 2014. Modeling the water-bottom geometry effect on peak time shifting in Lidar bathymetric waveforms. IEEE Geosci. Remote Sens. Lett. 11, pp.1285–1289. doi:10.1109/LGRS.2013.2292814

Guenther, G.C., Cunningham, A.G., LaRocque, P.E., Reid, D.J., 2000. Meeting the accuracy challenge in airborne bathymetry (No. ADA488934). National Oceanic Atmospheric Administration/Nesdis Silver Spring MD.

Jethra, R., 1993. Turbidity measurement. ISA Trans. 32, pp.397–405. doi:10.1016/0019-0578(93)90075-8

Kinzel, P.J., Legleiter, C.J., Nelson, J.M., 2013. Mapping river bathymetry with a small footprint green Lidar: applications and challenges. JAWRA J. Am. Water Resour. Assoc. 49, pp.183–204. doi:10.1111/jawr.12008

O'Dell, J.W., 1993. Method 180.1: Determination of turbidity by nephelometry (Revision 2.0). Office of Research and Development, U.S. Environmental Protection Agency, Cincinnati, OH.

Pan, Z., Glennie, C., Hartzell, P., Fernandez-Diaz, J., Legleiter, C., Overstreet, B., 2015. Performance assessment of high resolution airborne full waveform Lidar for shallow river bathymetry. Remote Sens. 7, pp. 5133–5159. doi:10.3390/rs70505133

Quan, X., Fry, E.S., 1995. Empirical equation for the index of refraction of sea water. Appl. Opt. 34, 3477. doi:10.1364/AO.34.003477

Saylam, K., 2016. A tale of two airborne Lidar scanners— lower Colorado River basin survey. Lidar Mag. 6, pp.34–37.

Saylam, K., 2009. Quality assurance of Lidar systems: mission planning, in: American Society of Photogrametry and Remote Sensing Conference. Presented at the ASPRS 2009, Curran Associates, Baltimore, MD, pp. 9–13.

Saylam, K., Brown, R.A., Hupp, J.R., 2017. Assessment of depth and turbidity with airborne Lidar bathymetry and multiband satellite imagery in shallow water bodies of the Alaskan North Slope. Int. J. Appl. Earth Obs. Geoinformation 58, pp.191–200. doi:10.1016/j.jag.2017.02.012

Sinjin, E., Roger, C., 2015. American rivers' 10 most endangered rivers for 2015 (Yearly report). American Rivers.

USGS, 2016. USGS current conditions for the Nation: Colorado River below Parker Dam, USGS 09427520 [Online document]. https://waterdata.usgs.gov/nwis/uv?

Wang, C., Li, Q., Liu, Y., Wu, G., Liu, P., Ding, X., 2015. A comparison of waveform processing algorithms for single-wavelength Lidar bathymetry. ISPRS J. Photogramm. Remote Sens. 101, pp. 22–35. doi:10.1016/j.isprsjprs.2014.11.005